

RESEARCH ARTICLE

Open Access



# Radiomics signature for dynamic changes of tumor-infiltrating CD8+ T cells and macrophages in cervical cancer during chemoradiotherapy

Kang Huang<sup>1,2†</sup>, Xuehan Huang<sup>1,3†</sup>, Chengbing Zeng<sup>1†</sup>, Siyan Wang<sup>1,3</sup>, Yizhou Zhan<sup>1</sup>, Qingxin Cai<sup>1</sup>, Guobo Peng<sup>1</sup>, Zhining Yang<sup>1</sup>, Li Zhou<sup>4</sup>, Jianzhou Chen<sup>1,5,6\*</sup> and Chuangzhen Chen<sup>1\*</sup> 

## Abstract

**Background** Our previous study suggests that tumor CD8+ T cells and macrophages (defined as CD68+ cells) infiltration underwent dynamic and heterogeneous changes during concurrent chemoradiotherapy (CCRT) in cervical cancer patients, which correlated with their short-term tumor response. This study aims to develop a CT image-based radiomics signature for such dynamic changes.

**Methods** Thirty cervical squamous cell carcinoma patients, who were treated with CCRT followed by brachytherapy, were included in this study. Pre-therapeutic CT images were acquired. And tumor biopsies with immunohistochemistry at primary sites were performed at baseline (0 fraction (F)) and immediately after 10F. Radiomics features were extracted from the region of interest (ROI) of CT images using Matlab. The LASSO regression model with ten-fold cross-validation was utilized to select features and construct an immunomarker classifier and a radiomics signature. Their performance was evaluated by the area under the curve (AUC).

**Results** The changes of tumor-infiltrating CD8+T cells and macrophages after 10F radiotherapy as compared to those at baseline were used to generate the immunomarker classifier (AUC= 0.842, 95% CI:0.680–1.000). Additionally, a radiomics signature was developed using 4 key radiomics features to predict the immunomarker classifier (AUC=0.875, 95% CI:0.753-0.997). The patients stratified based on this signature exhibited significant differences in treatment response ( $p = 0.004$ ).

**Conclusion** The radiomics signature could be used as a potential predictor for the CCRT-induced dynamic alterations of CD8+ T cells and macrophages, which may provide a less invasive approach to appraise tumor immune status during CCRT in cervical cancer compared to tissue biopsy.

**Keywords** Radiomics signature, CD8+ T cells, Macrophages, Immunomarker classifier, Concurrent chemoradiotherapy

<sup>†</sup>Kang Huang, Xuehan Huang and Chengbing Zeng contributed equally to this work and should be considered co-first authors.

\*Correspondence:

Jianzhou Chen  
cjzeoeo@gmail.com  
Chuangzhen Chen  
czchen2@stu.edu.cn

Full list of author information is available at the end of the article



© The Author(s) 2024. **Open Access** This article is licensed under a Creative Commons Attribution 4.0 International License, which permits use, sharing, adaptation, distribution and reproduction in any medium or format, as long as you give appropriate credit to the original author(s) and the source, provide a link to the Creative Commons licence, and indicate if changes were made. The images or other third party material in this article are included in the article's Creative Commons licence, unless indicated otherwise in a credit line to the material. If material is not included in the article's Creative Commons licence and your intended use is not permitted by statutory regulation or exceeds the permitted use, you will need to obtain permission directly from the copyright holder. To view a copy of this licence, visit <http://creativecommons.org/licenses/by/4.0/>. The Creative Commons Public Domain Dedication waiver (<http://creativecommons.org/publicdomain/zero/1.0/>) applies to the data made available in this article, unless otherwise stated in a credit line to the data.

## Introduction

The tumor microenvironment (TME) refers to the internal and external environment of tumor cells, including abundant infiltrating immune cells along with inflammatory cytokines. The TME plays an important role in the growth and metastasis of tumors. Recently, a considerable amount of evidence has demonstrated that immune status is closely associated with tumor progression and the patient's prognosis [1–7]. A previous study showed that the number of infiltrating neutrophils was correlated with infiltrating CD8+ T cells in muscle-invasive urinary bladder cancer. Also, high infiltration of neutrophils is associated with an immunosuppressive state, shorter survival time, and poor clinical outcomes [5]. In patients with high-grade glioma, a decrease of CD4+ T-cells and an increase of regulatory T cells drive resistance towards immunotherapy [2]. Moreover, most identified biomarkers reflect the immune characteristics of TME [8]. Among them, tumor-infiltrating immune cells and expression of immune-related molecules had been confirmed to be effective biomarkers reflecting the status of the TME [9, 10]. High expression levels of immune checkpoints might suggest an immunosuppressive TME resulting in tumor cell evasion of immune attack [11]. Thus, immune-related biomarkers of the TME are associated with tumor prognostic outcomes and therapeutic efficacy.

Traditionally, surgery, chemotherapy, and radiotherapy are the main clinical treatments for malignant tumors. Besides killing tumor cells directly, radiation therapy (RT) can activate the immune response of patients through multiple mechanisms, including the generation of neoantigens, activation of dendritic cells, and production of interferon. In addition, immunotherapy has advanced in recent years, especially immune checkpoint blockade (ICB) therapy, which has emerged as the main therapeutic option for cancer [12–15]. Hence, when RT enhances immune responses and turns cold tumors into hot tumors by changing the TME, ICB may improve the overall therapeutic efficacy when combined with RT [16]. Unfortunately, only a small proportion of patients benefit from the combination of ICB and RT [17–19]. One of the main reasons may be the lack of immune infiltration in TME, the so-called “cold tumor” [20].

In our previous study, the population of CD8+ T lymphocytes in TME exhibited different trends before and after 10F radiotherapy in cervical cancer (CC). High CD8+ T cells infiltration was correlated with increased IRF1 expression in the nucleus of tumor cells and better short-term outcomes, and there was a positive association between the expression of PD-L1 and IRF1 in tumor cells. The tumor-infiltrating macrophages (defined as CD68+ cells) also displayed heterogeneous responses

to concurrent chemoradiotherapy (CCRT) [21]. Thus, evaluation of the immune cell infiltration in TME and the immune-related gene expression during chemoradiotherapy may predict the therapeutic response and help select subgroups of patients that are more likely to benefit from immunotherapy.

Because tumor-associated immune responses happen in a short duration after RT, prompt tissue biopsies obtained at various times may be required to reveal the changes in the TME [22]. As the most common gynecologic tumor, CC serves as an ideal model to approach this problem, characterized by its strong immunogenicity and relative accessibility for biopsy. So, we developed an immunomarker classifier by screening 13 immune biomarkers in CC before treatment and after 10F of radiotherapy. The biomarker expression has to be determined by immunohistochemistry performed after tissue sample extraction, and the focal lesion gradually shrinks or even disappears after radiotherapy and/or chemotherapy. These limit its clinical application. Therefore, a non-invasive, timely, and efficient predictor for this immunomarker classifier is needed.

As an emerging technique, radiomics have been mainly applied in the early diagnosis, differential diagnosis [23, 24], staging [25, 26], prognosis, and treatment evaluation [27–31] of tumors, which have demonstrated improved diagnostic and predictive performance compared to conventional imaging techniques. It is found that radiomics could also effectively predict the immune status [32, 33]. Concentrating on the fields of radiomics and oncology [34–36], we believe that radiomics has the potential to predict this immunomarker classifier. To our knowledge, a radiomics signature based on immune scores for assessment of the infiltration of immune cells in TME and the expressions of immune checkpoint genes has not been well established.

In this study, we identified the biomarkers and established an immunomarker classifier by using mathematical models to evaluate the CCRT-induced alterations in CD8+ T cells and macrophages. Furthermore, we built a radiomics signature based on this immune model to assess the dynamic changes in tumor-infiltrating CD8+ T cells and macrophages in CC patients during CCRT.

## Methods

### Study design and patients

The study enrolled a cohort of 30 consecutive patients treated at the Cancer Hospital of Shantou University Medical College. All these patients matched the following inclusion criteria: (a) pathologically confirmed primary cervical squamous cell carcinoma (FIGO stages IB3, IIA2, IIB-IVA); (b) received CCRT; (c) standard contrast-enhanced pelvic CT and MRI scans performed

within 14 days before CCRT; (d) availability of primary tumor biopsy during the period of CCRT. The exclusion criteria were as follows: (a) history of antitumor therapy (immunotherapy and radiotherapy that would cause overlapping of planned radiotherapy fields); (b) history of autoimmune diseases; (c) concurrent immunotherapy during radiotherapy; (d) contraindications for biopsy; (e) tumor lesions could not be distinguished by CT.

Enrolled patients received external beam radiation therapy (EBRT) and platinum-based concurrent chemotherapy followed by brachytherapy (see detailed regimens in the [supplement](#)). Before treatment, patients underwent essential examinations including tumor biopsy, blood tests and other examinations for tumor staging and pretreatment assessment. Another tumor biopsy and complete blood count were obtained instantly after 10F of radiotherapy. Cervical biopsies were obtained from the superior portion of the ectocervix using biopsy forceps (2-5 pieces, no less than 2\*2 mm tissue). After the whole course of pelvic EBRT, short-term response to CCRT in patients was evaluated in accordance with the RECIST 1.0 version. Complete response (CR) was defined as the absence of cervical lesions as assessed by the bimanual examination. Partial response (PR) was defined as at least a 30% decrease in the lesion maximum diameter compared with the baseline.

Clinical and hematological data, such as age, FIGO staging, platelet count (PLT), absolute neutrophil count (ANC), absolute monocyte count (AMC), and absolute lymphocyte count (ALC), were derived from medical records. The neutrophil-lymphocyte ratio (NLR) was calculated as the ratio of ANC to ALC, platelet neutrophil ratio (PNR) as the ratio of APC to ANC, platelet lymphocyte ratio (PLR) as the ratio of APC to ALC, and lymphocyte monocyte ratio (LMR) as the ratio of ALC to AMC. Using the receiver operating characteristic (ROC) curves and the Youden Index, the optimal cutoff scores for hematological features were determined based on their association with the response to the CCRT. The size of the primary tumor and LN status were recorded in the clinical radiological report. Patients with visible regional LN > 1cm in the maximal short-axis diameter and/or clusters of  $\geq 3$  lymph nodes were identified as clinically LN-positive.

The FIGO staging was classified according to the revised 2018 International Federation of Gynecology and Obstetrics (FIGO) staging system for CC. Ethical approval was obtained from the clinical study ethics committee in the Cancer Hospital of Shantou University Medical College (Shantou, P.R. China), and all patients were informed consent. This study complied with the Declaration of Helsinki.

### IHC staining and construction of immunomarker classifier

Immunohistochemical staining and evaluation were processed as previously described [21]. We calculated the changes of expression of 13 immune biomarkers after 10F-RT, including infiltrating CD8+T cells, infiltrating CD68+ cells, and 11 IFN-responsive molecules (PD-L1, SERPINB9, CD47, nuclear IRF1, nuclear STAT1, HLA-A, HLA-B/C,  $\beta$ 2M, TAP1, LMP2 and LMP7) in tumor cells. The least absolute shrinkage and selection operator (LASSO) regression model was used to determine the most useful predictive features out of all the 13 immune features, and then we generated a multi-immune markers-based classifier to predict patients' response to CCRT [37]. To demonstrate the stability of this model, we applied internal ten-fold cross-validation [38, 39]. The LASSO logistic regression model was analyzed with the "glmnet" R package.

### CT acquisition and VOI delineation

The pretreatment contrast-enhanced computed tomography scan (Philips Brilliance CT Big Bore Oncology Configuration, Cleveland, OH, USA; voxel size:  $1.0 \times 1.0 \times 5.0$  mm; scan voltage: 120 kV; convolution kernel: Philips Healthcare's B) was conducted for each patient. Patients received a cubital vein injection of iodinated contrast agent (IODAMEPOLE, 70-80ml, 1.8-2.0ml/s, 22-25s) prior to scanning. Portal venous-phase images were transmitted to Varian Eclipse TPS (Treatment Planning System), and then the volume of interest (VOI) was segmented by a senior radiation oncologist with 15 years of experience. In our study, the VOI covered the entire gross volume of the primary tumor and the whole uterus.

### Feature extraction, selection, and radiomics signature construction

From the VOI of each patient, a total of 97 image features were extracted using in-house software implemented in MATLAB (version R2016a, MathWorks, Natick, USA). The radiomics features could be separated into 3 types: 24 intensity CT features, 20 geometric, and 53 textural features (detail in [supplementary](#)). We found that the ranges of different features were varied, and hence the imaging data were standardized with zero-mean normalization (Z-score) to avoid the potential effect on the classification performance. Firstly, univariate regression analysis was used to evaluate the predictive performance of each radiomics feature, and only the features with  $p < 0.2$  were selected for intensive study. Secondly, we used the LASSO model with 10-fold cross-validation to further select the features with non-zero coefficients and

construct a radiomics signature to predict the previous immunomarker classifier.

**Statistical analysis**

Continuous variables were compared using the Student’s t-test (normally distributed) or Wilcoxon rank-sum test (nonnormally distributed). The Chi-square test was utilized to compare the differences in categorical variables. All clinical variables were evaluated with univariate logistic regression analyses, and multivariate logistic regression was performed to determine the significant independent factors of treatment benefit. The discrimination of the immunomarker classifier and radiomics signature was quantified with the receiver operator characteristic (ROC) curve. Statistical analysis was conducted using R software (version 4.0.5), jamovi software (version 1.6.23), and SPSS software (version 23.0). A two-sided *p*-value < 0.05 was regarded as statistically significant.

**Results**

**Clinical characteristics**

The detailed clinical characteristics of the cohort were summarized in Table 1. All enrolled patients were well tolerated, and no patient presented with a diagnosis of malnutrition or urinary tract infection throughout the duration of the trial. Of the 30 patients included in the study, 17 (56.7%) were evaluated as CR after CCRT, and the rest of 13 (43.3%) were assessed as PR. We used the receiver operating characteristic (ROC) curves and the Youden Index to select the optimal cutoff points for all 8 hematological features (Supplementary Fig. S1, S2) and classified them into low and high groups. Between the CR and PR groups, there were statistically significant differences in FIGO stage, tumor size, pre-NLR, pre-PLR, pre-LMR, 10F-PNR, 10F-PLR, and 10F-LMR (*p* < 0.05). However, age, LN metastasis, pre-PNR and 10F-NLR showed no significant differences (Table 1).

**Development and validation of immunomarker classifier**

The univariate regression analysis of immune features was listed in Supplementary Table S1, which indicated that the infiltrating CD8+T cells were the most significant variable in predicting response to CCRT in CC patients. The changes in the number of infiltrating CD8+T cells and CD68+ cells were selected to build the final immunomarker-based classifier by using the LASSO logistic regression model with ten-fold cross-validation (Fig. 1A, 1B). The classifier showed a satisfying discriminatory efficacy for treatment response with AUCs of 0.842 (95% CI, 0.680-1.000) (Fig. 1C). The model score for each patient was calculated according to the following formula: immune score = 0.4569 + 0.0041 × (CD8+T cell at 10F minus that at baseline)

**Table 1** Characteristics of patients according to the treatment response

Variables	Response		p
	PR (n = 13)	CR (n = 17)	
<b>Age (years)</b>			0.177
<60	10 (76.9%)	9 (52.9%)	
≥60	3 (23.1%)	8 (47.1%)	
<b>FIGO stage</b>			0.030 *
I~II	4 (30.8%)	12 (70.6%)	
III~IV	9 (69.2%)	5 (29.4%)	
<b>Tumor size (cm)</b>			0.020 *
<4	1 (7.7%)	8 (47.1%)	
≥4	12 (92.3%)	9 (52.9%)	
<b>LN metastasis</b>			0.153
Negative	5 (38.5%)	11 (64.7%)	
Positive	8 (61.5%)	6 (35.3%)	
<b>Pre-NLR</b>			0.009 *
Low	1 (7.7%)	9 (52.9%)	
High	12 (92.3%)	8 (47.1%)	
<b>Pre-PNR</b>			0.225
Low	9 (69.2%)	8 (47.1%)	
High	4 (30.8%)	9 (52.9%)	
<b>Pre-PLR</b>			0.004 *
Low	4 (30.8%)	14 (82.4%)	
High	9 (69.2%)	3 (17.6%)	
<b>Pre-LMR</b>			0.003 *
Low	7 (53.8%)	1 (5.9%)	
High	6 (46.2%)	16 (94.1%)	
<b>10F-NLR</b>			0.127
Low	4 (30.8%)	10 (58.8%)	
High	9 (69.2%)	7 (41.2%)	
<b>10F-PNR</b>			0.012 *
Low	4 (30.8%)	13 (76.5%)	
High	9 (69.2%)	4 (23.5%)	
<b>10F-PLR</b>			0.013 *
Low	6 (46.2%)	15 (88.2%)	
High	7 (53.8%)	2 (11.8%)	
<b>10F-LMR</b>			0.004 *
Low	10 (76.9%)	4 (23.5%)	
High	3 (23.1%)	13 (76.5%)	
<b>Immune score, median (interquartile range)</b>	0.042 (-0.264 to 0.278)	0.548 (0.416 to 0.749)	0.002 *

Tumor size and LN metastasis were evaluated by a radiologist according to patient’s MRI before treatment

Abbreviations: LN metastasis Lymph nodes metastasis, Pre-NLR Neutrophil lymphocyte ratio before treatment, Pre-PNR Platelet neutrophil ratio before treatment, Pre-PLR Platelet lymphocyte ratio before treatment, Pre-LMR Lymphocyte monocyte ratio before treatment, 10F-NLR Neutrophil lymphocyte ratio after 10F RT, 10F-PNR Platelet neutrophil ratio after 10F RT, 10F-PLR Platelet lymphocyte ratio after 10F RT, 10F-LMR Lymphocyte monocyte ratio after 10F RT

Significance: \* *p* value < 0.05

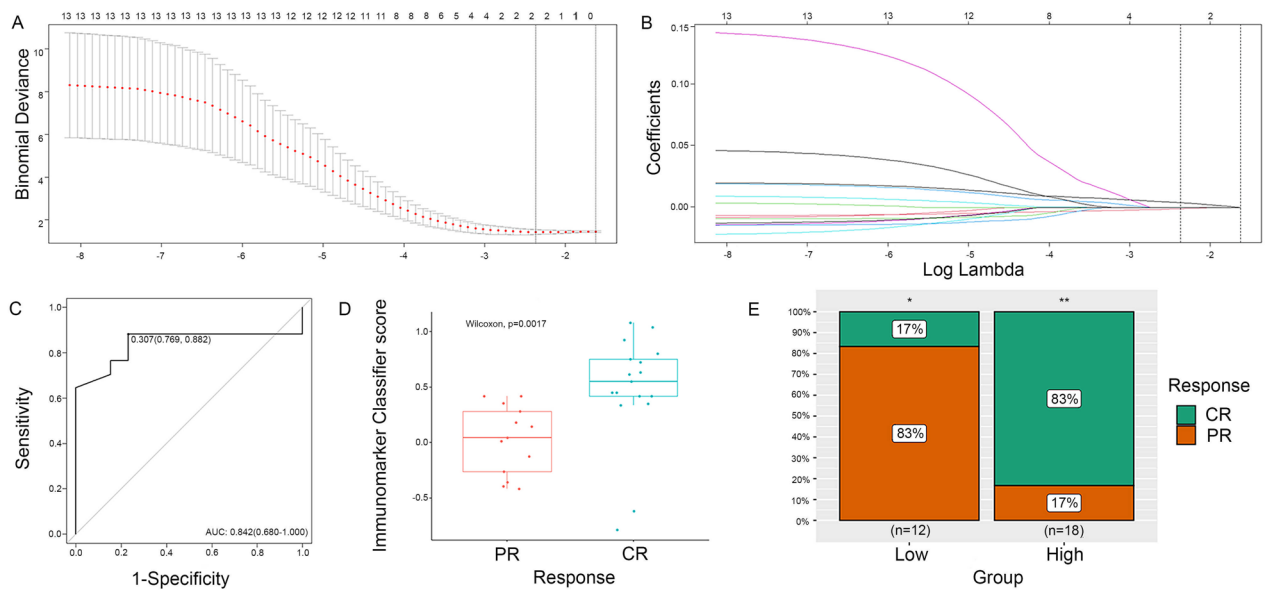


**Fig. 1** Feature selection and construction of the immunomarker classifier using LASSO logistic regression, and the predictive performance of the classifier. **A** Tuning parameter ( $\lambda$ ) selection in the LASSO model via ten-fold cross-validation based on minimum criteria. The binomial deviance was plotted versus  $\log(\lambda)$ . The dotted vertical line was set with minimum criteria, and the optimal  $\lambda$  value of 0.094 with  $\log(\lambda)$  of -2.368 was selected. **B** LASSO coefficient profiles of the 13 immune markers. A vertical line was drawn at the value selected by 10-fold cross-validation, where optimal  $\lambda$  resulted in 2 features with nonzero coefficients. **C** ROC curve and Youden's index of the Immunomarker Classifier. **D** The immune score boxplots between complete and partial remission groups. **E** Comparison of the immediate responses between the low-score group and the high-score group. Significance: \*  $p$  value < 0.05. \*\* $p$  < 0.01

- 0.0009  $\times$  (CD68+ cell at 10F minus that at baseline), and the immune scores (median [interquartile range]) in patients with CR after CCRT were significantly higher than those with PR (0.548 [0.416 to 0.749] vs. 0.042 [-0.264 to 0.278], respectively,  $p = 0.0017$ ) (Table 1 and Fig. 1D). As displayed in Fig. 1C, the optimal cut-off for classifier scores determined by Youden's index was 0.307, and the model had a sensitivity of 0.882 while obtaining a specificity of 0.769, respectively. Accordingly, patients could be divided into two groups: low-score group (score < 0.307) and high-score group (score  $\geq$  0.307). The low-score group consisted of 12 patients, in which 2/12 (17%) were evaluated as CR and 10/12 (83%) as PR. For the high-score group, 15/18 (83%) patients were considered as CR, and the remaining 3/18 (17%) as PR. High-score patients had a significantly higher CR rate than low-score patients ( $p < 0.001$ ) (Fig. 1E).

We performed univariate binary logistic regression analysis to evaluate the ability of clinical features to distinguish therapy response. As shown in Table 2, the AUC values of this immunomarker-based model were higher than any single clinical variable, which suggested that this classifier achieved the best predictive efficacy. Multivariate logistic regression was performed adjusting for clinical variables and it suggested that the immunomarker

classifier score was an independent predictor of treatment response (Table 2).

**Construction and performance of radiomics signature**

Of all 97 radiomics features extracted from VOI, there were 36 features meeting the criterion that  $p < 0.2$  in univariate analysis. LASSO regression algorithm with ten-fold cross-validation, a common regression model for high-dimensional data, was utilized to further determine the most significant 4 imaging features and develop a radiomics signature to discriminate immunomarker classifier. An AUC of 0.875 (95% CI, 0.753-0.997) revealed that the radiomics signature had a great ability to distinguish the high-score group from the low-score group (Fig. 2A). Fig. 2B showed that the radiomics signature also exhibited good discrimination for therapy response with AUCs of 0.864 (95% CI, 0.734-0.994). The radiomics signature and 10F-LMR were identified as independent factors of treatment response in CC patients by multivariate regression analysis (Supplementary Table S2).

The calculated formula of the radiomics score was shown in the supplementary. There were significant differences between the radiomics score (median [interquartile range]) in immunomarker groups (-0.175 [-1.450 to 0.371] vs. 1.320 [0.519 to 1.490], respectively,  $p = 0.0003$ ) and response groups (-0.452 [-1.450 to

**Table 2** Risk factors for treatment response in cervical cancer

Variable	Univariate Logistic Regression			Multivariate Logistic Regression	
	OR (95% CI)	p	AUC	OR (95% CI)	p
<b>Immune score</b> (per 0.1 increase)	12.267 (1.493-100.770)	0.020 *	0.842	32.448 (1.430-735.592)	0.029 *
<b>Age (years)</b> (<60 vs. ≥60)	2.963 (0.596-14.730)	0.184	0.620	NA	NA
<b>FIGO stage</b> (I~II vs. III~IV)	0.185 (0.038-0.893)	0.036 *	0.699	NA	NA
<b>Tumor size (cm)</b> (<4 vs. ≥4)	0.094 (0.010-0.891)	0.039 *	0.697	NA	NA
<b>LN metastasis</b> (Negative vs. Positive)	0.341 (0.076-1.522)	0.159	0.631	NA	NA
<b>Pre-NLR</b> (Low vs. High)	0.074 (0.008-0.704)	0.023 *	0.726	NA	NA
<b>Pre-PNR</b> (Low vs. High)	2.531 (0.557-11.512)	0.229	0.611	NA	NA
<b>Pre-PLR</b> (Low vs. High)	0.095 (0.017-0.529)	0.007 *	0.758	NA	NA
<b>Pre-LMR</b> (Low vs. High)	18.667 (1.879-185.406)	0.012 *	0.740	36.366 (1.050-1255.634)	0.047 *
<b>10F-NLR</b> (Low vs. High)	0.311 (0.068-1.430)	0.133	0.640	NA	NA
<b>10F-PNR</b> (Low vs. High)	0.137 (0.027-0.695)	0.016 *	0.729	NA	NA
<b>10F-PLR</b> (Low vs. High)	0.114 (0.018-0.716)	0.020 *	0.710	NA	NA
<b>10F-LMR</b> (Low vs. High)	10.833 (1.961-59.836)	0.006 *	0.767	20.348 (1.100-377.655)	0.043 *

Abbreviations: NA Not available, LN metastasis Lymph nodes metastasis, Pre-NLR Neutrophil lymphocyte ratio before treatment, Pre-PNR Platelet neutrophil ratio before treatment, Pre-PLR Platelet lymphocyte ratio before treatment, Pre-LMR Lymphocyte monocyte ratio before treatment, 10F-NLR Neutrophil lymphocyte ratio after 10F RT, 10F-PNR Platelet neutrophil ratio after 10F RT, 10F-PLR platelet lymphocyte ratio after 10F RT, 10F-LMR Lymphocyte monocyte ratio after 10F RT

Significance: \*  $p$  value < 0.05

0.595] vs. 1.320 [0.512 to 1.530], respectively,  $p = 0.0004$ ) (Figs. 2C and 2D). The optimal cut-off value of radiomics score determined by ROC curve analysis was 1.036, and patients were classified into low-Radscore group (Radscore < 1.036) and high-Radscore group (Radscore ≥ 1.036). The low-Radscore group included 19 patients, in which fewer patients received CR but there is no significant difference (37% vs. 63%,  $p > 0.05$ ). As for the high-Radscore group, most patients were evaluated as CR (91% vs. 9%,  $p < 0.01$ ). It indicated that treatment response was significantly different for patients stratified by radiomics signature ( $p = 0.004$ ) (Fig. 2E).

## Discussion

Tumor progression and response to therapy are associated with TME. It has been reported that chemoradiotherapy could exert anti-tumor efficiency by altering the TME [40–42]. Similarly, our previous study showed that the variations of innate immune markers during the treatment course displayed a closer relation to the efficacy of CCRT for CC, demonstrating that the alternations in the TME resulting from chemoradiotherapy may be an important factor for affecting patient prognosis and therapeutic response. In this study, we proposed an immunomarker classifier to appraise the alterations in TME-related biomarkers during therapy in CC patients, and a corresponding radiomics signature was created.

Based on the clinical research data from our previous trial (NCT03744819), we analyzed the changes of the expression of 13 immune markers before and after 10

sessions of radiotherapy, selected the most useful predictive features via the LASSO algorithm with ten-fold cross-validation, and developed a new immunomarker classifier. Patients with lower immune scores had a lower CR rate, indicating the immune score may be a poor prognostic factor. We also confirmed that the robust value of the immunomarker classifier was an independent predictor of treatment response. Furthermore, compared with the FIGO staging system, which was widely used to guide treatment strategy for CC, this immunomarker classifier could provide additional information about the infiltration of immune cells and show good predictive ability.

In this study, the immunomarker classifier was determined by the number of changes in CD8+ T cells and CD68+ cells in the TME during CCRT. CD8+ T cells are cytotoxic T lymphocytes that secrete various cytokines to exert their antitumor effect [43]. CD68 is a specific surface marker of macrophages. CD8+ T cells and tumor-associated macrophages (TAMs) are the predominant immune population in the TME. Although macrophages have several function phenotypes, the majority of macrophages tend to acquire the M2 phenotype and facilitate tumor growth and metastasis [44, 45]. A study demonstrated that the infiltrating lymphocyte percentage in breast cancer was an independent predictor of the efficacy of neoadjuvant chemotherapy [46]. Another study on lung cancer found that tumor-infiltrating lymphocytes were associated with the efficacy of immune checkpoint inhibitors

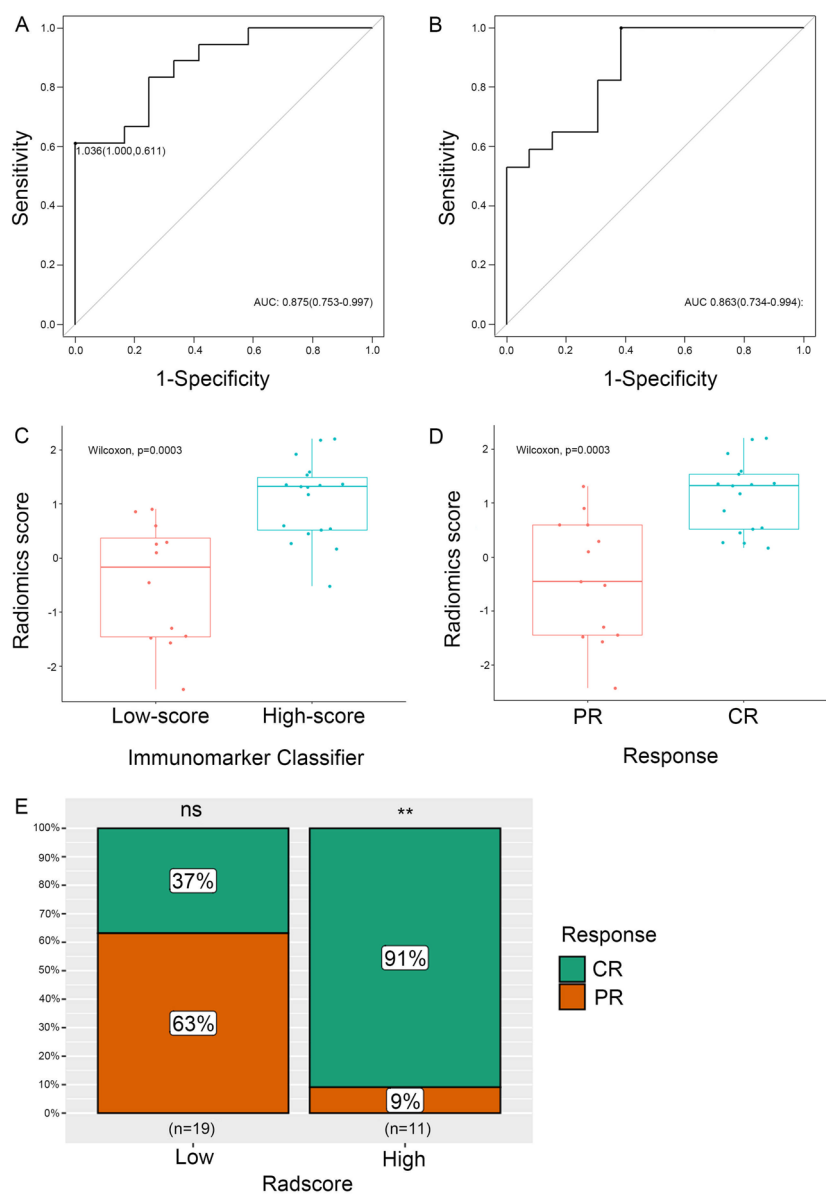


**Fig. 2** Construction and predictive performance of the radiomics signature using LASSO logistic regression. **A** ROC curves of the Radiomics Signature to predict Immunomarker Classifier. **B** ROC curves of the Radiomics Signature to predict treatment response. **C** The radiographic scores boxplots between the high-score immune group and the low-score group. **D** The radiographic scores boxplots between complete and partial remission groups. **E** Comparison of the immediate responses between the low-Radscore group and the high-Radscore group. Significance: ns = not significant, \*\* $p < 0.01$

[47]. Besides, among patients with advanced colorectal cancer who had received bevacizumab plus irinotecan/oxaliplatin-based combination chemotherapy, those with lower TAM infiltration showed two times longer overall survival compared to those with higher TAM infiltration [48]. These findings suggest that infiltrating lymphocytes play a fundamental role in anti-tumor immune response and prognosis, while TAMs favor tumor progression.

The same trend was found in this study. Patients with higher scores had increased CD8+ T cells and decreased CD68+ cells after CCRT in the TME which we had termed immune-inflamed TME (i.e., “hot” tumor). And vice versa, patients with lower scores had an immunosuppressive TME (i.e., “cold” tumor). In short, CC patients could be divided into two different groups based on the immunomarker classifier score for predicting the immune infiltration to guide individualized treatment.

In the present work, we performed a tumor biopsy before and after 10F radiotherapy to evaluate the changes in the expression of the biomarkers related to the TME. This approach has the advantage of discovering the immuno-phenotype changes and the molecular changes during chemoradiotherapy. Hence, our immunomarker classifier calculated immune scores by analyzing changes in the number of CD8+ T cells and macrophages between pre- and post-treatment comprehensively.

The detection of immune-related biomarkers in TME requires biopsies which is not feasible in most disease types and is a lack of compliance in patients with accessible tumors. Radiomics is currently in development and can explore diagnostic and prognostic information by extracting tumor features quantitatively from medical images in the field of tumor research which may solve this problem [49]. Currently, several studies have investigated the relationship between radiomics signatures and TME. The above-mentioned study by Sun et al [32], and Jiang et al [50] found that radiomics signatures could reflect the immune state and the characteristics of the TME. In this study, we tried to establish the radiomics signature in CC via CT to predict the immunomarker classifier. At the same time, we found that the radiomics signature could identify CC patients who have a better treatment response, and the patients with higher radiomics scores had a significantly higher CR rate than those with lower radiomics scores.

In recent years, immunotherapy represented by immune checkpoint blockade (ICB) has been a significant advance in the treatment of various tumors. Nevertheless, only a small part of patients display improved responses from the PD-L1 blockade or even RT and ICB combined therapy. Consequently, aiding the identification of patients suitable for immunotherapy by assessing the immune status following chemoradiation therapy is necessary to avoid overtreatment and unnecessary economic burden. The result of the present study demonstrated that the high-Radscore group displayed increased CD8 + T cells infiltration and decreased macrophages infiltration in the TME after 10F-RT, meaning that patients were in an immunocompetent state, while the low-Radscore group had the opposite result. We envisaged that the dynamic modifications of the tumor-infiltrating immune cells in patients may be predicted by performing contrast-enhanced pelvic CT during chemoradiotherapy. It is a potential tool in guiding individualized treatment regimens for cancer patients.

This study had several limitations. Firstly, this was a single-center study and the data set was not divided into training and testing cohorts due to the limited sample size. Ten-fold cross-validation was used to internally verify to reduce model errors and prevent overfitting. Thus,

further large clinical research is warranted. Secondly, it has been reported that M1 and M2 macrophages co-exist in TME [51]. CD68 cannot distinguish between two phenotypes but is rather a pan-macrophage marker. Further experiments are needed to discriminate the impact of two phenotypes, such as flow cytometry and single-cell sequencing.

## Conclusions

In conclusion, the immunomarker classifier could assess CD8+ T cells and macrophages infiltration in TME during CCRT in CC. The radiomics signature could predict the immune score to evaluate the dynamic changes in the infiltration of CD8+ T cells and macrophages during CCRT. Additionally, the radiomics signature might be a potential predictive tool to guide the stratification of treatment strategies and achieve treatment individualization for patients.

## Abbreviations

AUC	Area Under Curve
CCRT	Concurrent chemoradiotherapy
CT	Computed Tomography
EBRT	External beam radiation therapy
FIGO	International Federation of Gynecology and Obstetrics
ICB	Immune checkpoint blockade
LASSO	Least Absolute Shrinkage and Selection Operator
MRI	Magnetic Resonance Imaging
RECIST	Response Evaluation Criteria in Solid Tumors
ROC	Receiver operating characteristic curve
TAM	Tumor-associated macrophage
VOI	Volume of interest

## Supplementary Information

The online version contains supplementary material available at <https://doi.org/10.1186/s40644-024-00680-0>.

### Additional file 1: Supplementary Methods and Results. Table S1.

Univariate logistic regression analysis for immune features. Table S2.

Independent predictors for treatment response in cervical cancer. Fig. S1.

ROC curves and Youden Index of hematological features before treatment.

Fig. S2. ROC curves and Youden Index of hematological features after 10F RT.

## Acknowledgements

Not applicable.

## Authors' contributions

Research idea and study design: K.H., C.Z., J.C., C.C. Data acquisition: K.H., C.Z., Y.Z., Q.C., G.P., Z.Y., L.Z. Data analysis/interpretation: K.H., X.H., C.Z. Supervision or mentorship: J.C., C.C., S.W.

## Funding

This study was funded by the Clinical Research Project of the Cancer Hospital of Shantou University Medical College, 2023B001 (to CC); the Natural Science Foundation of Guangdong Province of China, 2022A1515220007 (to CC); the Innovative Research Group Project of the National Natural Science Foundation of China, 82173079 (to JC and CC); the Natural Science Foundation of Guangdong Province of China, 2022A1515011220 (to JC and CC); the Shantou Science and Technology Plan Medical and Health Category Project, 210408216492660 (to YZ and CC); the Shantou Science and Technology Plan Medical and Health Category Project, 230509116495546 (to QC and CC); the Shantou University Medical College Clinical Research Enhancement

Initiative, N0201424 (to CC and JC); the Science and Technology Special Fund of Guangdong Province of China, 2019-132 (to CC); the Strategic and Special Fund for Science and Technology Innovation of Guangdong Province of China, 180918114960704 (to CC); the Science and Technology Bureau of Shantou, 200110115871710 (to LZ).

#### Availability of data and materials

The datasets used and/or analysed during the current study are available from the corresponding author on reasonable request.

#### Declarations

#### Ethics approval and consent to participate

The Ethics Committee of Cancer Hospital of Shantou University Medical College approved this study.

#### Consent for publication

Not applicable.

#### Competing interests

The authors declare that they have no competing interests.

#### Author details

<sup>1</sup>Department of Radiation Oncology, Cancer Hospital of Shantou University Medical College, Shantou, P.R. China. <sup>2</sup>Department of Radiation Oncology, Zhongshan City People's Hospital, Zhongshan, P.R. China. <sup>3</sup>Shantou University Medical College, Shantou, P.R. China. <sup>4</sup>Department of Gynecologic Oncology, Cancer Hospital of Shantou University Medical College, Shantou, China. <sup>5</sup>Gustave Roussy Cancer Campus, Villejuif Cedex, France. <sup>6</sup>Institut National de la Santé Et de la Recherche Médicale (INSERM) U1015, Équipe Labellisée - Ligue Nationale contre le Cancer, Villejuif, France.

Received: 23 November 2023 Accepted: 28 February 2024

Published online: 23 April 2024

#### References

- Angell H, Galon J. From the immune contexture to the Immunoscore: the role of prognostic and predictive immune markers in cancer. *Curr Opin Immunol.* 2013;25(2):261–7.
- Aslan K, Turco V, Blobner J, Sonner JK, Liuzzi AR, Nunez NG, et al. Heterogeneity of response to immune checkpoint blockade in hypermutated experimental gliomas. *Nat Commun.* 2020;11(1):931.
- Pages F, Mlecnik B, Marliot F, Bindea G, Ou FS, Bifulco C, et al. International validation of the consensus Immunoscore for the classification of colon cancer: a prognostic and accuracy study. *Lancet.* 2018;391(10135):2128–39.
- Jiang Y, Zhang Q, Hu Y, Li T, Yu J, Zhao L, et al. ImmunoScore signature: a prognostic and predictive tool in gastric cancer. *Ann Surg.* 2018;267(3):504–13.
- Zhou L, Xu L, Chen L, Fu Q, Liu Z, Chang Y, et al. Tumor-infiltrating neutrophils predict benefit from adjuvant chemotherapy in patients with muscle invasive bladder cancer. *Oncoimmunology.* 2017;6(4):e1293211.
- Fridman WH, Pages F, Sautès-Fridman C, Galon J. The immune contexture in human tumours: impact on clinical outcome. *Nat Rev Cancer.* 2012;12(4):298–306.
- Galon J, Pages F, Marincola FM, Angell HK, Thurin M, Lugli A, et al. Cancer classification using the Immunoscore: a worldwide task force. *J Transl Med.* 2012;10:205.
- Muhitch JB, Hoffend NC, Azabdafari G, Miller A, Bshara W, Morrison CD, et al. Tumor-associated macrophage expression of interferon regulatory Factor-8 (IRF8) is a predictor of progression and patient survival in renal cell carcinoma. *J Immunother Cancer.* 2019;7(1):155.
- Bruni D, Angell HK, Galon J. The immune contexture and Immunoscore in cancer prognosis and therapeutic efficacy. *Nat Rev Cancer.* 2020;20(11):662–80.
- Autio M, Leivonen SK, Bruck O, Mustjoki S, Meszaros Jorgensen J, Karjalainen-Lindsberg ML, et al. Immune cell constitution in the tumor microenvironment predicts the outcome in diffuse large B-cell lymphoma. *Haematologica.* 2021;106(3):718–29.
- Wang C, Tang Y, Ma H, Wei S, Hu X, Zhao L, et al. Identification of hypoxia-related subtypes, establishment of prognostic models, and characteristics of tumor microenvironment infiltration in colon cancer. *Front Genet.* 2022;13:919389.
- Gupta A, Probst HC, Vuong V, Landshammer A, Muth S, Yagita H, et al. Radiotherapy promotes tumor-specific effector CD8+ T cells via dendritic cell activation. *J Immunol.* 2012;189(2):558–66.
- Reits EA, Hodge JW, Herberts CA, Groothuis TA, Chakraborty M, Wansley EK, et al. Radiation modulates the peptide repertoire, enhances MHC class I expression, and induces successful antitumor immunotherapy. *J Exp Med.* 2006;203(5):1259–71.
- Harding SM, Benci JL, Irianto J, Discher DE, Minn AJ, Greenberg RA. Mitotic progression following DNA damage enables pattern recognition within micronuclei. *Nature.* 2017;548(7668):466–70.
- Deng L, Liang H, Xu M, Yang X, Burnette B, Arina A, et al. STING-dependent cytosolic DNA sensing promotes radiation-induced type I interferon-dependent antitumor immunity in immunogenic tumors. *Immunity.* 2014;41(5):843–52.
- McLaughlin M, Patin EC, Pedersen M, Wilkins A, Dillon MT, Melcher AA, et al. Inflammatory microenvironment remodelling by tumour cells after radiotherapy. *Nat Rev Cancer.* 2020;20(4):203–17.
- Antonia SJ, Villegas A, Daniel D, Vicente D, Murakami S, Hui R, et al. Overall survival with durvalumab after chemoradiotherapy in stage III NSCLC. *N Engl J Med.* 2018;379(24):2342–50.
- Formenti SC, Rudqvist NP, Golden E, Cooper B, Wennerberg E, Lhuillier C, et al. Radiotherapy induces responses of lung cancer to CTLA-4 blockade. *Nat Med.* 2018;24(12):1845–51.
- Luke JJ, Lemons JM, Karrison TG, Pitroda SP, Melotek JM, Zha Y, et al. Safety and clinical activity of pembrolizumab and multisite stereotactic body radiotherapy in patients with advanced solid tumors. *J Clin Oncol.* 2018;36(16):1611–8.
- Bonaventura P, Shekarian T, Alcazer V, Valladeau-Guilemond J, Valsesia-Wittmann S, Amigorena S, et al. Cold tumors: a therapeutic challenge for immunotherapy. *Front Immunol.* 2019;10:168.
- Chen J, Chen C, Zhan Y, Zhou L, Chen J, Cai Q, et al. Heterogeneity of IFN-mediated responses and tumor immunogenicity in patients with cervical cancer receiving concurrent chemoradiotherapy. *Clin Cancer Res.* 2021;27(14):3990–4002.
- Kelly RJ, Zaidi AH, Smith MA, Omstead AN, Kosovec JE, Matsui D, et al. The dynamic and transient immune microenvironment in locally advanced esophageal adenocarcinoma post chemoradiation. *Ann Surg.* 2018;268(6):992–9.
- Beig N, Khorrami M, Alloum M, Prasanna P, Braman N, Orooji M, et al. Perinodular and intranodular radiomic features on lung CT images distinguish adenocarcinomas from granulomas. *Radiology.* 2019;290(3):783–92.
- Lambin P, Rios-Velazquez E, Leijenaar R, Carvalho S, van Stiphout RG, Granton P, et al. Radiomics: extracting more information from medical images using advanced feature analysis. *Eur J Cancer.* 2012;48(4):441–6.
- Wang X, Sun W, Liang H, Mao X, Lu Z. Radiomics signatures of computed tomography imaging for predicting risk categorization and clinical stage of thymomas. *Biomed Res Int.* 2019;2019:3616852.
- Qian Z, Li Y, Wang Y, Li L, Li R, Wang K, et al. Differentiation of glioblastoma from solitary brain metastases using radiomic machine-learning classifiers. *Cancer Lett.* 2019;451:128–35.
- Zhai TT, van Dijk LV, Huang BT, Lin ZX, Ribeiro CO, Brouwer CL, et al. Improving the prediction of overall survival for head and neck cancer patients using image biomarkers in combination with clinical parameters. *Radiother Oncol.* 2017;124(2):256–62.
- Hu Y, Xie C, Yang H, Ho JWK, Wen J, Han L, et al. Assessment of intratumoral and peritumoral computed tomography radiomics for predicting pathological complete response to neoadjuvant chemoradiation in patients with esophageal squamous cell carcinoma. *JAMA Netw Open.* 2020;3(9):e2015927.
- Xie D, Wang TT, Huang SJ, Deng JJ, Ren YJ, Yang Y, et al. Radiomics nomogram for prediction disease-free survival and adjuvant chemotherapy benefits in patients with resected stage I lung adenocarcinoma. *Transl Lung Cancer Res.* 2020;9(4):1112–23.

30. Nie K, Shi L, Chen Q, Hu X, Jabbour SK, Yue N, et al. Rectal cancer: assessment of neoadjuvant chemoradiation outcome based on radiomics of multiparametric MRI. *Clin Cancer Res.* 2016;22(21):5256–64.
31. Wang T, Gao T, Guo H, Wang Y, Zhou X, Tian J, et al. Preoperative prediction of parametrial invasion in early-stage cervical cancer with MRI-based radiomics nomogram. *Eur Radiol.* 2020;30(6):3585–93.
32. Sun R, Limkin EJ, Vakalopoulou M, Dercle L, Champiat S, Han SR, et al. A radiomics approach to assess tumour-infiltrating CD8 cells and response to anti-PD-1 or anti-PD-L1 immunotherapy: an imaging biomarker, retrospective multicohort study. *Lancet Oncol.* 2018;19(9):1180–91.
33. Jiang Y, Chen C, Xie J, Wang W, Zha X, Lv W, et al. Radiomics signature of computed tomography imaging for prediction of survival and chemotherapeutic benefits in gastric cancer. *EBioMedicine.* 2018;36:171–82.
34. Luo LM, Huang BT, Chen CZ, Wang Y, Su CH, Peng GB, et al. A combined model to improve the prediction of local control for lung cancer patients undergoing stereotactic body radiotherapy based on radiomic signature plus clinical and dosimetric parameters. *Front Oncol.* 2021;11:819047.
35. Liu W, Zeng C, Wang S, Zhan Y, Huang R, Luo T, et al. A combined predicting model for benign esophageal stenosis after simultaneous integrated boost in esophageal squamous cell carcinoma patients (GASTO1072). *Front Oncol.* 2022;12:1026305.
36. Peng G, Zhan Y, Wu Y, Zeng C, Wang S, Guo L, et al. Radiomics models based on CT at different phases predicting lymph node metastasis of esophageal squamous cell carcinoma (GASTO-1089). *Front Oncol.* 2022;12:988859.
37. Tibshirani R. Regression Shrinkage and Selection Via the Lasso. *J Royal Stat Soc Series B (Methodological).* 1996;58(1):267–88.
38. Breiman L, Spector PC. Submodel selection and evaluation in regression The X-random case. *Int Stat Rev.* 1992;60:291–319.
39. Kohavi R. A study of cross-validation and bootstrap for accuracy estimation and model selection. *Proceedings of the 14th international joint conference on Artificial intelligence - Volume 2*; Montreal: Morgan Kaufmann Publishers Inc.; 1995. p. 1137–43.
40. Herter JM, Kiljan M, Kunze S, Reinscheid M, Ibruli O, Cai J, et al. Influence of chemoradiation on the immune microenvironment of cervical cancer patients. *Strahlenther Onkol.* 2023;199(2):121–30.
41. Hassanian H, Asadzadeh Z, Baghbanzadeh A, Derakhshani A, Dufour A, Rostami Khosroshahi N, et al. The expression pattern of Immune checkpoints after chemo/radiotherapy in the tumor microenvironment. *Front Immunol.* 2022;13:938063.
42. van den Ende T, van den Boorn HG, Hoonhout NM, van Etten-Jamaludin FS, Meijer SL, Derks S, et al. Priming the tumor immune microenvironment with chemo(radio)therapy: A systematic review across tumor types. *Biochim Biophys Acta Rev Cancer.* 2020;1874(1):188386.
43. Hossain MA, Liu G, Dai B, Si Y, Yang Q, Wazir J, et al. Reinvigorating exhausted CD8(+) cytotoxic T lymphocytes in the tumor microenvironment and current strategies in cancer immunotherapy. *Med Res Rev.* 2021;41(1):156–201.
44. Yan S, Wan G. Tumor-associated macrophages in immunotherapy. *FEBS J.* 2021;288(21):6174–86.
45. Xiang X, Wang J, Lu D, Xu X. Targeting tumor-associated macrophages to synergize tumor immunotherapy. *Signal Transduct Target Ther.* 2021;6(1):75.
46. Denkert C, Loibl S, Noske A, Roller M, Muller BM, Komor M, et al. Tumor-associated lymphocytes as an independent predictor of response to neoadjuvant chemotherapy in breast cancer. *J Clin Oncol.* 2010;28(1):105–13.
47. Tang H, Wang Y, Chlewicki LK, Zhang Y, Guo J, Liang W, et al. Facilitating T cell infiltration in tumor microenvironment overcomes resistance to PD-L1 blockade. *Cancer Cell.* 2016;29(3):285–96.
48. Dost Gunay FS, Kirmizi BA, Ensari A, Icli F, Akbulut H. Tumor-associated macrophages and neuroendocrine differentiation decrease the efficacy of bevacizumab plus chemotherapy in patients with advanced colorectal cancer. *Clin Colorectal Cancer.* 2019;18(2):e244–50.
49. Mayerhoefer ME, Materka A, Langs G, Haggstrom I, Szczypinski P, Gibbs P, et al. Introduction to Radiomics. *J Nucl Med.* 2020;61(4):488–95.
50. Jiang Y, Wang H, Wu J, Chen C, Yuan Q, Huang W, et al. Noninvasive imaging evaluation of tumor immune microenvironment to predict outcomes in gastric cancer. *Ann Oncol.* 2020;31(6):760–8.
51. Kusano T, Ehirchiou D, Matsumura T, Chobaz V, Nasi S, Castelblanco M, et al. Targeted knock-in mice expressing the oxidase-fixed form of xanthine oxidoreductase favor tumor growth. *Nat Commun.* 2019;10(1):4904.

## Publisher's Note

Springer Nature remains neutral with regard to jurisdictional claims in published maps and institutional affiliations.